Biosensors and Bioelectronics 34 (2012) 227–231

Contents lists available at SciVerse ScienceDirect

Biosensors and Bioelectronics

journal homepage: www.elsevier.com/locate/bios

Label-free colorimetric sensor for ultrasensitive detection of heparin based on color quenching of gold nanorods by graphene oxide

Xiuli Fu[a,c], Lingxin Chen[a,*], Jinhua Li[a], Meng Lin[a], Huiyan You[b], Wenhai Wang[a]

[a] Key Laboratory of Coastal Zone Environmental Processes, Yantai Institute of Coastal Zone Research, Chinese Academy of Sciences, Yantai 264003, China
[b] Environmental and Chemical Engineering College, Dalian University, Dalian 116622, China
[c] Graduate University of Chinese Academy of Sciences, Beijing 100049, China

ARTICLE INFO

Article history:
Received 1 December 2011
Received in revised form 5 February 2012
Accepted 6 February 2012
Available online 15 February 2012

Keywords:
Heparin
Gold nanorods
Graphene oxide
Colorimetric detection

ABSTRACT

A novel label-free colorimetric strategy was developed for ultrasensitive detection of heparin by using the super color quenching capacity of graphene oxide (GO). Hexadecyltrimethylammonium bromide (CTAB)-stabilized gold nanorods (AuNRs) could easily self-assembly onto the surface of GO through electrostatic interaction, resulting in decrease of the surface plasmon resonance (SPR) absorption and consequent color quenching change of the AuNRs from deep to light. Polycationic protamine was used as a medium for disturbing the electrostatic interaction between AuNRs and GO. The AuNRs were prevented from being adsorbed onto the surface of GO because of the stronger interaction between protamine and GO, showing a native color of the AuNRs. On the contrary, in the presence of heparin, which was more easily to combine with protamine, the AuNRs could self-assembly onto the surface of GO, resulting in the native color disappearing of AuNRs. As the concentration of heparin increased, the color of AuNRs would gradually fade until almost colorless. The amounts of self-assembly AuNRs were proportional to the concentration of heparin, and thereby the changes in the SPR absorption and color had been used to monitor heparin levels. Under optimized conditions, good linearity was obtained in a range of 0.02–0.28 μg/mL (R = 0.9957), and a limit of detection was 5 ng/mL. The simultaneous possession of high sensitivity and selectivity, simplicity, rapidity, and visualization enabled this sensor to be potentially applicable for ultrasensitive and rapid on-site detection toward trace heparin.

1. Introduction

Heparin is a highly negatively charged polysaccharide due to the sulphate and carboxylate residues (Casu, 1985; Rabenstein, 2002). It has been widely used as the anticoagulant during numerous surgical procedures involving extracorporeal blood circulation such as cardiopulmonary bypass surgery (Jaques, 1979; Mulloy and Linhardt, 2001). However, the overdose of heparin often causes potentially fatal bleeding complication (Hirsh, 1984). Hence, close monitoring of heparin levels is extremely important to avoid the risk such as hemorrhage and thrombocytopenia, especially for pediatric patients.

Recently, various techniques and methods have been established for the determination of heparin. For examples, a chromo-fluorogenic sensing platform based on silica nanoparticles was developed, for the detection of heparin (Climent et al., 2009). A multicolor biosensor for heparin detection and quantification was developed on the basis of the fluorescence change of a water-soluble 2,1,3-benzothiadiazole-containing cationic conjugated polymer (Pu and Liu, 2008, 2009). Determination of heparin was completed based on heparin coated poly(methyl methacrylate) (PMMA) intraocular lenses by ion chromatography (Ander et al., 2001). And a reversed-phase ion pair high-performance liquid chromatography (RPIP-HPLC) was developed for the separation of heparins using a C_{18} column (Patel et al., 2009). However, these methods are usually restricted to complex instruments, time-consuming procedure, or low sensitivity. Therefore, it is urgently required to develop simple, fast, sensitive and cost-effective methods.

Colorimetric methods are extremely attractive because they offer advantages of low-cost portable instruments and simple operation process; moreover, they can be easily read out with naked eyes (Carey et al., 2011; Laurieri et al., 2010; Li et al., 2011; Lou et al., 2011). Noble metal nanomaterials, in particular, gold nanorods (AuNRs), have attracted much attention in colorimetric detection due to their interesting physical and chemical properties (Castellana et al., 2011; Kuo et al., 2010; Liu et al., 2011). AuNRs show higher absorption cross sections and stronger light scattering properties than those of spherical gold nanoparticles owing to their stronger surface plasmon resonance (SPR) characteristics (Liao and

* Corresponding author. Tel.: +86 535 2109130; fax: +86 535 2109130.
E-mail address: lxchen@yic.ac.cn (L. Chen).

0956-5663/$ – see front matter © 2012 Elsevier B.V. All rights reserved.
doi:10.1016/j.bios.2012.02.008

Hafner, 2005; Parab et al., 2010). The major advantage of the AuNRs-based colorimetric assay is that it exhibits two SPR bands: one is the transverse band, corresponding to electron oscillation along the short axis of AuNRs; the other is the longitudinal band, corresponding to electron oscillation along the long axis of AuNRs (Parab et al., 2010). The longitudinal SPR band can be tuned from the visible to the near-infrared region of the electromagnetic spectrum along with the changes of molar extinction coefficients, by adjusting the aspect ratio of the AuNRs (Orendorff and Murphy, 2006). Moreover, the longitudinal SPR band of AuNRs has been found to be very sensitive to changes in the local environment, including solvent, substrate, adsorbate and interparticle distances (Parab et al., 2010). Therefore, the AuNRs-based colorimetric assay has extremely high sensitivity, and has been widely applied for the detection of various analytes including DNA (He et al., 2008), peptides (Sudeep et al., 2005), cancer cells (Jiang et al., 2011; Park et al., 2009), etc. Recently, we have used mesoporous silica-coated AuNRs to attain high sensitive and selective colorimetric detection of Hg^{2+}, S^{2-} and ascorbic acid (Wang et al., 2011a, 2011b).

Graphene oxide (GO) is a monolayer of two dimensional carbon-based materials containing multi-functional groups such as carboxyl, epoxy, ketone and hydroxyl groups in its basal and edge planes (Dreyer et al., 2010). GO has shown great potential for biological applications because of its good water dispersibility, high mechanical strength, versatile surface modification, and photoluminescence (Geim, 2009; Stankovich et al., 2006). Due to the ability of quenching fluorescence (Lu et al., 2009; Wen et al., 2010), GO has been widely applied to DNA analysis (Liu et al., 2010), pathogen detection (Jung et al., 2010) and protein assay (Chang et al., 2010). Lately, GO has also been used for the effective adsorption of cationic dyes based on the large negative charge density (Ramesha et al., 2011). However, to the best of our knowledge, to date there are few reports about the use of GO to quench the color of nanoparticles for efficient detection of biomolecules based on the self-assembly through electrostatic interaction.

Herein, we proposed a new colorimetric strategy for ultrasensitive detection of heparin based on GO quenching the color of self-assembly AuNRs. Hexadecyltrimethylammonium bromide (CTAB)-stabilized AuNRs were chosen for monitoring changes in the color and the SPR absorptions to investigate the concentrations of heparin. The specificity of this system was assured through the strong affinity of protamine for heparin. Thus, a rapid, simple, low-cost, visual and label-free colorimetric assay was developed for ultrasensitive and selective detection of heparin.

2. Experimental

2.1. Chemicals and materials

Graphene oxide was purchased from Nanjing XFNano Materials Technology Company. Protamine sulfate salt was obtained from Sigma–Aldrich. Heparin sodium salt from bovine intestinal mucosa was purchased from Aladdin Chemistry Co. Ltd (185 U/mg, Shanghai, China). Hyaluronic acid (HA) salt was obtained from Streptococcus equi (BioChemika). Chondroitin sulfate (Chs) was purchased from Aladdin Chemistry Co. Ltd (Shanghai, China). DNA was provided by Shanghai Shenggong Co. (Shanghai, China). Glucose, cysteine, glutamic acid, aspartic acid, hexadecyltrimethylammonium bromide (CTAB), gold chloride trihydrate ($HAuCl_4{\cdot}3H_2O$), silver nitrate, sodium borohydride ($NaBH_4$), ascorbic acid and other affiliated reagents were all obtained from Sinopharm Chemical Reagent (Shanghai, China). 4-(2-Hydroxyethyl)-1-piperazineethanesulfonic acid (HEPES) buffer solution was used for all the experiments, adjusting with 1 M NaOH to reach pH 7.4. All chemicals and reagents were of analytical grade or better. Aqueous solutions were prepared with freshly deionized water (18.2 MΩ specific resistance) obtained with a Pall Cascada laboratory water system.

2.2. Synthesis of gold nanorods

AuNRs were synthesized following the seed-mediated and CTAB surfactant-directed method according to that reported (Nikoobakht and El-Sayed, 2003) with necessary modification. Briefly, the seed solution was prepared by mixing 2.5 mL of CTAB (0.2 M) and 2.5 mL of $HAuCl_4$ (0.6 mM) aqueous solutions. Subsequently, to the stirred solution, 0.30 mL of freshly prepared ice-cold $NaBH_4$ solution (0.01 M) was added, resulting in the color of the solution changing from yellow to brown. The obtained solution was stirred for another 2 min and stored as the seed solution for the synthesis of AuNRs.

80 mL of CTAB solution (0.10 M), 1.2 mL of $HAuCl_4$ (50 mM) solution and 0.055–0.33 mL of $AgNO_3$ solution (50 mM) were mixed at room temperature. Then 1 mL of 0.080 M ascorbic acid was added with gentle stirring. Ascorbic acid as a mild reducing agent, only for the reduction of gold ions, changed the growth solution from dark yellow to colorless. It should be noted that solutions were identical except for their Ag^+ content. AuNRs with different longitudinal plasmon bands could be acquired by controlling the aspect ratios via adjusting the addition amounts of $AgNO_3$ (Jiang et al., 2011; Nikoobakht and El-Sayed, 2003).

Finally, 0.16 mL of the seed solution was added to the growth solution. The mixed solution was left undisturbed for at least 20 h at 28 °C. Excess CTAB was removed by centrifuging twice at 8000 rpm. The supernatant solution was discarded and the resultant particles were re-dispersed in pure water.

2.3. Instrumentation

Absorption spectra were recorded at room temperature on a Thermo Scientific NanoDrop 2000/2000C spectrophotometer (USA) using a 1 cm quartz cell. Atomic force microscopy (AFM) images of GO were recorded on a freshly cleaved mica surface by using a Nanoscope V multimode atomic force microscope (Veeco Instruments, USA) in tapping mode. Transmission electron microscopy (TEM) images were obtained by a JEM-1230 electron microscope (JEOL, Ltd., Japan) operating under 100 kV accelerating voltage.

2.4. Sample preparation

0.05 μg/mL protamine solution was prepared using HEPES buffer (pH 7.4, 10 mM). Various contents of heparin (0–160 μL, 0.002 mg/mL) were mixed with protamine solution, maintaining a gentle stirring for 5 min. The mixture was incubated for another 5 min with the addition of 60 μL of GO solution (0.01 mg/mL), allowing for the left protamine to be completely adsorbed onto the GO surface. Subsequently, 200 μL of AuNRs were added into the above solutions. After incubation for 5 min, the UV–visible (UV–vis) absorption spectra were recorded.

3. Results and discussion

3.1. Sensing principle for heparin

As GO has large numbers of negative charges and CTAB-stabilized AuNRs contain numerous positive charges, the AuNRs can easily self-assembly on the surface of GO through electrostatic interaction. The AuNRs which we used not only could be attached to the surface of GO, but also possessed interesting optical properties arising from localized surface plasmon resonances (Quintana et al., 2010). Protamine, a kind of polycation with ~20 positive charges

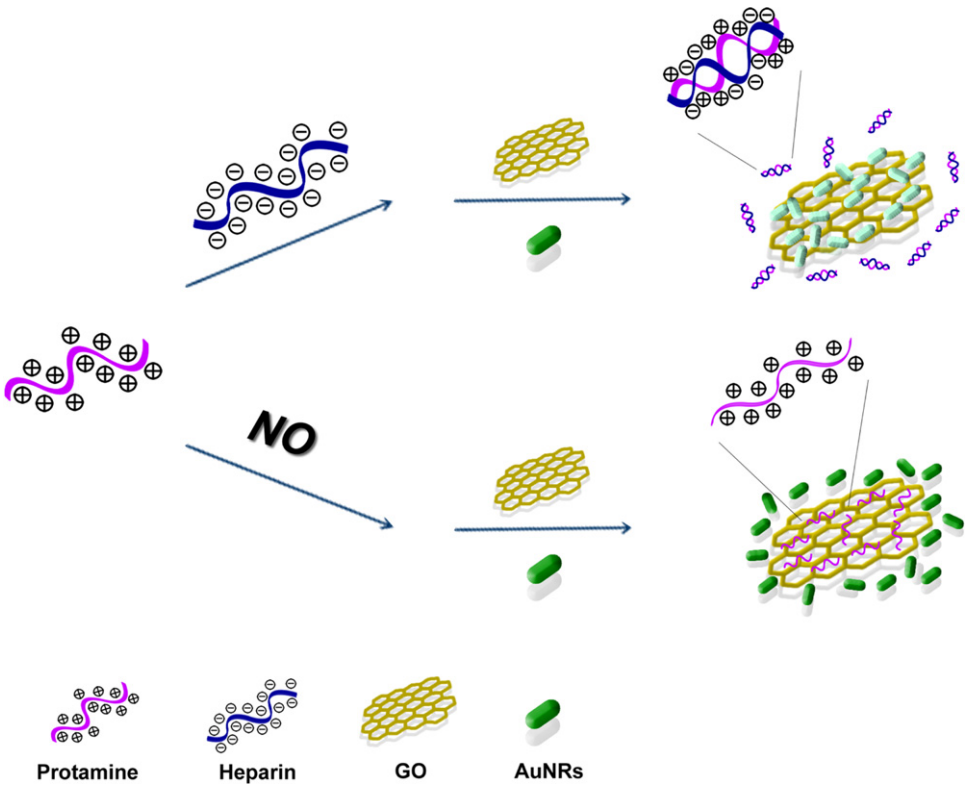

Fig. 1. Schematic illustration of GO quenching the color of AuNRs sensing heparin based on the self-assembly of CTAB-stabilized AuNRs on the surface of GO.

due to its abundance in basic arginine residue, could result in the tight electrostatic binding of polyanionic heparin to form a stable complex (Jena and Raj, 2008; Kim and Rose, 1995; Shvarev and Bakker, 2003). Based on the strong affinity of protamine for heparin, it was chosen as a medium to detect heparin. As illustrated in Fig. 1, in the existence of polyanionic heparin, protamine was hybridized with heparin first, and the AuNRs could self-assembly onto the surface of GO through electrostatic interaction, resulting in the decrease in the SPR absorption and the native color quenching of AuNRs. On the contrary, in the absence of polyanionic heparin, GO was more easily combined with protamine. Consequently, the AuNRs were prevented from being adsorbed onto the surface of GO, displaying an intense SPR absorption and thereby native color appearing. Thus the changes in the SPR absorption of AuNRs were expected to provide a quantitative readout for heparin.

3.2. Optical characterization

To demonstrate the strategy, the ability of GO as a platform for quenching the color of AuNRs was first investigated. As shown in Fig. S1A, the thickness of GO was about 1.3 nm, which was reasonable for single layer GO. The thin nanoplate motif of GO was further examined by TEM (Fig. S1B), which exhibited the typical wrinkle morphology of GO. As seen in Fig. S2A, TEM image revealed that the AuNRs were in shape and size with an average length and aspect ratio of about 52 nm and 2.5:1, respectively. Initially, the CTAB-stabilized AuNRs were well dispersed in solution, showing both the transverse and the longitudinal plasmon resonance peaks at 512 and 637 nm, respectively (Fig. S2B) (Liao and Hafner, 2005), and the color of the uniform colloid was deep green (inset of Fig. S2B) due to its strong SPR absorption. After adding the negatively charged GO, AuNRs easily combined with GO because of the strong electrostatic interaction, resulting in the self-assembly of AuNRs and the color of the AuNRs colloid accordingly changed from deep to light with the decreasing of SPR absorption. As shown in Fig. S3A and S3C, with the concentration increase of GO, the absorbance of AuNRs gradually decreased along with the color gradually fading until colorless finally. The long axis of AuNRs was bound preferentially to the surface of GO, probably due to that the long axis of AuNRs had larger contact area than that of the short axis of AuNRs (Fig. S3B). Three different aspect ratios of AuNRs were prepared to certify this phenomenon further, and the results were consistent (Fig. S4). These observations indicated super color quenching ability of GO as well as strong self-assembly capacity of CTAB-stabilized AuNRs on GO.

As expected from the original design, protamine seriously disturbed the interaction between AuNRs and GO. Fig. 2A shows that the AuNRs were almost completely prevented from being adsorbed onto the surface of GO due to the stronger interaction between protamine and GO, remaining native color and displaying intense SPR absorption (inset photograph a and curve a). As expected, in the presence of polyanionic heparin, a significant decrease of the SPR absorption and the native color disappearing of AuNRs emerged (curve b and inset photograph b). This phenomenon was further evidenced by TEM images (Fig. 2B). More AuNRs were attached to the surface of GO (image b) when polyanionic heparin was added into the system, demonstrating that the heparin was more easily combined with protamine, and then the dispersed AuNRs could self-assembly onto the surface of GO through electrostatic interaction. On the other hand, without protamine, low SPR absorption of the AuNRs mixed with GO was observed, showing no obvious difference in the presence and absence of heparin (Fig. S5). All these results revealed that strong interaction of heparin and protamine facilitated AuNRs self-assembly on the surface of GO, and thereby induced to color quenching of AuNRs by GO, indicating great potential for quantitative analysis of heparin.

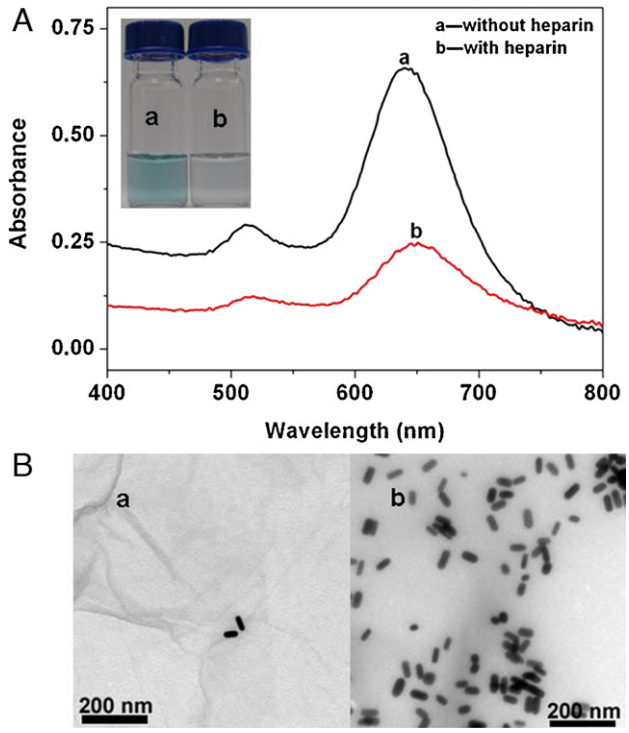

Fig. 2. (A) Absorption spectra and (B) TEM images of AuNRs in the GO/protamine mixed solutions in the absence (a) and presence (b) of heparin (0.24 μg/mL). Inset of part A: Photographic images of the corresponding colorimetric response (scale bars: 200 nm).

3.3. Optimization of experimental parameters

For optimization of the colorimetric strategy, potential effects of relevant experimental parameters, including concentrations of GO and protamine, and size of AuNRs were evaluated.

The effect of the GO concentration on the SPR absorption and the native color quenching of AuNRs was studied first. As described above, as the concentration of GO increased, the SPR absorption decreased and the native color of AuNRs gradually disappeared. This could be ascribed to that the increased amount of GO could adsorb more AuNRs. The interaction between GO and AuNRs was just like that between carbon nanotubes and polyelectrolytes (Kim and Sigmund, 2004; Rouse and Lillehei, 2003). The SPR absorption of AuNRs decreased rapidly with the concentration increase of GO until 0.6 μg/mL, and then tended to decrease slowly. Thus, 0.6 μg/mL GO was used in the following experiments.

Next, we further studied the effect of the amount of protamine for disturbing the interaction between AuNRs and GO. The higher the concentration of protamine was, the stronger interference was produced toward the interaction between AuNRs and GO. When the concentration of protamine reached 0.5 μg/mL, the AuNRs were almost completely prevented from being adsorbed onto the surface of GO (Fig. S6). Therefore, 0.5 μg/mL was chosen as the optimal concentration of protamine.

Finally, the effect of aspect ratio of AuNRs was investigated. Three different aspect ratios of AuNRs were tested including 1.8:1, 2.5:1 and 2.8:1. As seen from Fig. S7, the SPR response was proportional to the amount of heparin, and the AuNRs with the aspect ratio of 2.5:1 exhibited a higher sensitivity at 0.02 μg/mL of heparin and a wider concentration range of 0.02–0.32 μg/mL. For the other two aspect ratios, the overall profiles were similar to that for the aspect ratio of 2.5:1 but with a significantly lower sensitivity. Therefore, in order to obtain higher sensitivity and wider linear range, the aspect ratio of 2.5:1 for AuNRs was chosen.

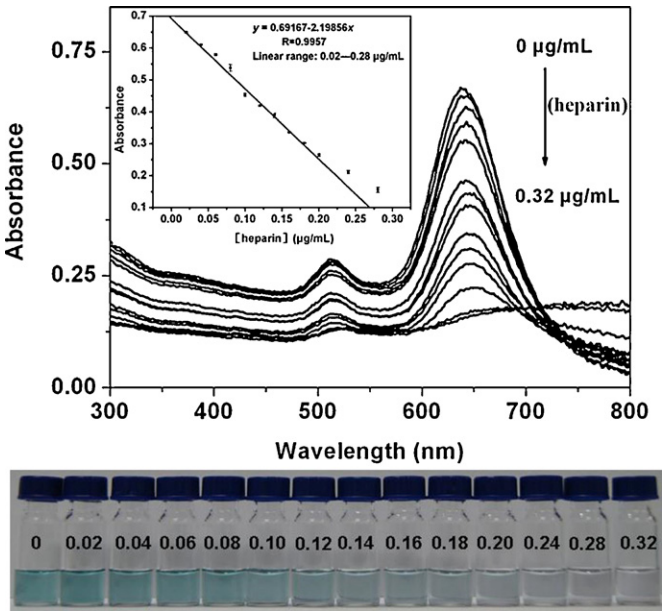

Fig. 3. (A) Absorption spectra of AuNRs in the GO/protamine mixed solution with various concentrations of heparin (0–0.32 μg/mL). Inset: the calibration curve of the GO-based system for the detection of heparin; error bars were obtained from five parallel experiments. (B) Photographic images of the corresponding colorimetric responses. From left to right: 0–0.32 μg/mL.

3.4. Performance of the colorimetric sensor

Under the optimized conditions, the UV–vis absorption spectra of AuNRs in the presence of heparin with different concentrations were recorded. Fig. 3 illustrated that the SPR absorbance of AuNRs at 513 and 637 nm gradually decreased with increasing concentration of heparin. The SPR absorbance change of AuNRs at 637 nm was more sensitive than that at 513 nm. The two SPR absorbance peaks are attributed to the transverse and the longitudinal plasmon resonance (Liao and Hafner, 2005). Due to the shape anisotropy of AuNRs, two well-defined types of resonances occurred, parallel and transversal to the long axis of the AuNRs (Jain et al., 2006). The sensitivity of the longitudinal plasmon band to interparticle interaction gave rise to strong changes in the absorption spectra, which was directly related to a plasmon coupling effect (Pramod and Thomas, 2008; Funston et al., 2009). Taking advantage of this behavior, the decreased 637 nm SPR absorption was employed to represent the amounts of self-assembly AuNRs, which was proportional to the concentration of heparin. The absorption values of AuNRs exhibited a good linear correlation to the concentration of heparin in the range of 0.02–0.28 μg/mL ($R = 0.9957$) (inset of Fig. 3A). Based on $3\sigma/s$ (σ is the standard deviation of the blank measurements and s is the sensitivity of the calibration graph), the detection limit of heparin was calculated to be 5 ng/mL. Such a value is at least one order of magnitude lower than that of the reported colorimetry for heparin as shown in Table S1. The improvement of the detection sensitivity was attributed to the significant absorbance decrease associated with the strong color quenching property of GO toward AuNRs in the presence of heparin.

3.5. Specificity of the sensor

To demonstrate the specificity for the detection of heparin on the GO-based colorimetric assay, competition experiments for selectivity to other molecules with similar molecular structures to heparin, and to commonly coexistent physiological level species, were further carried out. As shown in Fig. 4, in the presence of HA and Chs, the UV–vis absorption of AuNRs had a slight decrease

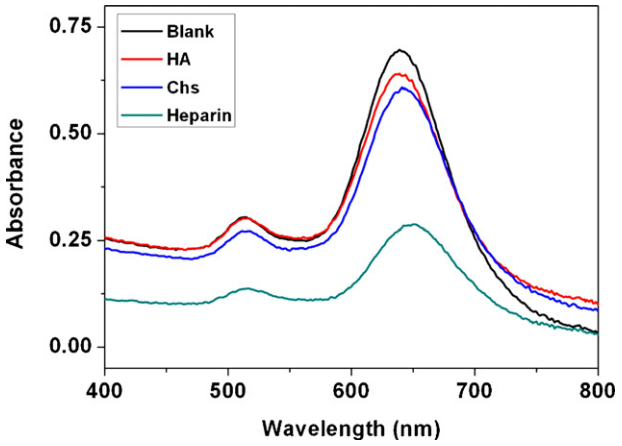

Fig. 4. Absorption spectra of AuNRs in the solutions of GO/protamine (black line), GO/protamine + 0.2 μg/mL HA (red line), GO/protamine + 0.2 μg/mL Chs (blue line), and GO/protamine + 0.2 μg/mL heparin (green line). (For interpretation of the references to color in this figure legend, the reader is referred to the web version of the article.)

compared to that given by the blank; interestingly, heparin led to a remarkable absorption decrease at an identical concentration with HA and Chs. This was simply due to the low charge density per repeat unit of HA and Chs, with only one carboxyl group and two groups of sulfate and carboxylate moieties, respectively. But heparin possesses three sulfate groups and one carboxylate per repeat unit (Dai et al., 2011). Thus, the electrostatic attraction between heparin and protamine was significantly stronger than that between HA–protamine and Chs–protamine. DNA was used as a model to investigate the effect of other polyanionic substances. The result showed that 50 ng/mL of DNA (plasma DNA normal level) did not interfere with the detection of heparin (Fig. S8). In addition, the general presence of physiological level species of Na^+, K^+, Mg^{2+}, Ca^{2+}, Cl^-, glucose, cysteine, glutamic acid and aspartic acid was also found not to affect the detection of heparin. It demonstrated that the developed program provided attractive specificity toward heparin.

4. Conclusions

In conclusion, a novel label-free colorimetric sensor was successfully developed for ultrasensitive detection of heparin based on GO quenching the color of self-assembly AuNRs. We took full advantage of the strong electrostatic interaction between GO and CTAB-stabilized AuNRs as well as high binding affinity of protamine with heparin, and thereby successfully attained the ultrasensitive detection of heparin with the detection limit of 5 ng/mL. The selective sensing system offered superiorities of label-free, simplicity, rapidity, visualization and high sensitivity for the detection of heparin. This assay strategy set an example of color quenching in analytical chemistry for the detection of polyionic analytes using nanotechnology, which also presaged potential applications in biological and environmental fields.

Acknowledgements

This work was financially supported by the National Natural Science Foundation of China (20975089, 21105117, 20875088), the Innovation Projects of the Chinese Academy of Sciences (KZCX2-EW-206), and the 100 Talents Program of the Chinese Academy of Sciences.

Appendix A. Supplementary data

Supplementary data associated with this article can be found, in the online version, at doi:10.1016/j.bios.2012.02.008.

References

Ander, B., Karlsson, A., Öhrlund, Å., 2001. J. Chromatogr. A 917, 105–110.
Carey, J.R., Suslick, K.S., Hulkower, K.I., Imlay, J.A., Imlay, K.R.C., Ingison, C.K., Ponder, J.B., Sen, A., Wittrig, A.E., 2011. J. Am. Chem. Soc. 133, 7571–7576.
Castellana, E.T., Gamez, R.C., Russell, D.H., 2011. J. Am. Chem. Soc. 133, 4182–4185.
Casu, B., 1985. Adv. Carbohydr. Chem. Biochem. 43, 51–134.
Chang, X.X., Tang, L.H., Wang, Y., Jiang, J.H., Li, J.H., 2010. Anal. Chem. 82, 2341–2346.
Climent, E., Calero, P., Marcos, M.D., Martínez-Máñez, R., Sancenón, F., Soto, J., 2009. Chem. Eur. J. 15, 1816–1820.
Dai, Q., Liu, W.M., Zhuang, X.Q., Wu, J.S., Zhang, H.Y., Wang, P.F., 2011. Anal. Chem. 83, 6559–6564.
Dreyer, D.R., Park, S., Bielawski, C.W., Ruoff, R.S., 2010. Chem. Soc. Rev. 39, 228–240.
Funston, A.M., Novo, C., Davis, T.J., Mulvaney, P., 2009. Nano Lett. 9, 1651–1658.
Geim, A.K., 2009. Science 324, 1530–1534.
He, W., Huang, C.Z., Li, Y.F., Xie, J.P., Yang, R.G., Zhou, P.F., Wang, J., 2008. Anal. Chem. 80, 8424–8430.
Hirsh, J., 1984. Nouv. Rev. Fr. Hematol. 26, 261–266.
Jain, P.K., Eustis, S., El-Sayed, M.A., 2006. J. Phys. Chem. B 110, 18243–18253.
Jaques, L.B., 1979. Pharmacol. Rev. 31, 99–166.
Jena, B.K., Raj, C.R., 2008. Biosens. Bioelectron. 23, 1285–1290.
Jiang, L., Qian, J., Cai, F., He, S., 2011. Anal. Bioanal. Chem. 400, 2793–2800.
Jung, J.H., Cheon, D.S., Liu, F., Lee, K.B., Seo, T.S., 2010. Angew. Chem. Int. Ed. 49, 5708–5711.
Kim, B., Sigmund, W.M., 2004. Langmuir 20, 8239–8242.
Kim, Y., Rose, C.A., 1995. Pharm. Res. 12, 1284–1288.
Kuo, T.R., Hovhannisyan, V.A., Chao, Y.C., Chao, S.L., Chiang, S.J., Lin, S.J., Dong, C.Y., Chen, C.C., 2010. J. Am. Chem. Soc. 132, 14163–14171.
Laurieri, N., Crawford, M.H.J., Kawamura, A., Westwood, I.M., Robinson, J., Fletcher, A.M., Davies, S.G., Sim, E., Russell, A.J., 2010. J. Am. Chem. Soc. 132, 3238–3239.
Li, J.H., Zhang, Z., Xu, S.F., Chen, L.X., Zhou, N., Xiong, H., Peng, H.L., 2011. J. Mater. Chem. 21, 19267–19274.
Liao, H.W., Hafner, J.H., 2005. Chem. Mater. 17, 4636–4641.
Liu, F., Choi, J.Y., Seo, T.S., 2010. Biosens. Bioelectron. 25, 2361–2365.
Liu, J.M., Wang, H.F., Yan, X.P., 2011. Analyst 136, 3904–3910.
Lou, T.T., Chen, Z.P., Wang, Y.Q., Chen, L.X., 2011. ACS Appl. Mater. Interfaces 3, 1568–1573.
Lu, C.H., Yang, H.H., Zhu, C.L., Chen, X., Chen, G.N., 2009. Angew. Chem. Int. Ed. 48, 4785–4787.
Quintana, M., Spyrou, K., Grzelczak, M., Browne, W.R., Rudolf, P., Prato, M., 2010. ACS Nano 4, 3527–3533.
Mulloy, B., Linhardt, R.J., 2001. Curr. Opin. Struct. Biol. 11, 623–628.
Nikoobakht, B., El-Sayed, M.A., 2003. Chem. Mater. 15, 1957–1962.
Orendorff, C.J., Murphy, C.J., 2006. J. Phys. Chem. B 110, 3990–3994.
Parab, H.J., Jung, C., Lee, J.H., Park, H.G., 2010. Biosens. Bioelectron. 26, 667–673.
Park, H., Lee, S., Chen, L., Lee, E.K., Shin, S.Y., Lee, Y.H., Son, S.W., Oh, C.H., Song, J.M., Kang, S.H., Choo, J., 2009. Phys. Chem. Chem. Phys. 11, 7444–7449.
Patel, R.P., Narkowicz, C., Jacobson, G.A., 2009. Anal. Biochem. 387, 113–121.
Pramod, P., Thomas, K.G., 2008. Adv. Mater. 20, 4300–4305.
Pu, K.Y., Liu, B., 2008. Macromolecules 41, 6636–6640.
Pu, K.Y., Liu, B., 2009. Adv. Funct. Mater. 19, 277–284.
Rabenstein, D.L., 2002. Nat. Prod. Rep. 19, 312–331.
Ramesha, G.K., Kumara, A.V., Muralidhara, H.B., Sampath, S., 2011. J. Colloid Interface Sci. 361, 270–277.
Rouse, J.H., Lillehei, P.T., 2003. Nano Lett. 3, 59–62.
Shvarev, A., Bakker, E., 2003. J. Am. Chem. Soc. 125, 11192–11193.
Stankovich, S., Dikin, D.A., Dommett, G.H.B., Kohlhaas, K.M., Zimney, E.J., Stach, E.A., Piner, R.D., Nguyen, S.T., Ruoff, R.S., 2006. Nature 442, 282–286.
Sudeep, P.K., Joseph, S.T.S., Thomas, K.G., 2005. J. Am. Chem. Soc. 127, 6516–6517.
Wang, G.Q., Chen, Z.P., Chen, L.X., 2011a. Nanoscale 3, 1756–1759.
Wang, G.Q., Chen, Z.P., Wang, W.H., Yan, B., Chen, L.X., 2011b. Analyst 136, 174–178.
Wen, Y.Q., Xing, F.F., He, S.J., Song, S.P., Wang, L.H., Long, Y.T., Li, D., Fan, C.H., 2010. Chem. Commun. 46, 2596–2598.